ELSEVIER

Fusion Engineering and Design 45 (1999) 465–474

Fusion Engineering and Design

www.elsevier.com/locate/fusengdes

Technical engineering note

Numerical study for design of the passive stabilizer and its impact on MHD stability in the proposed KSTAR plasma

D.-Y. Lee [a,*], C.S. Chang [a], J. Manickam [b], N. Pomphrey [b], M.S. Chance [b], S.C. Jardin [b]

[a] *Center for Plasma and Fusion Studies, Korea Advanced Institute of Science and Technology, 373-1 Kuseong-dong, Yuseong-ku, Taejon 305-701, South Korea*

[b] *Princeton Plasma Physics Laboratory, Princeton, NJ 08543, USA*

Received 4 May 1999; accepted 27 May 1999

Abstract

The effect of the passive plate stabilizer on the ideal magnetohydrodynamic (MHD) stability is numerically studied in order to guide its design in the proposed Korea Superconducting Tokamak Advanced Research (KSTAR). The parametric study is systematically performed by taking into account the two major variables: the plate's distance from the plasma surface, and the poloidal (toroidally continuous) vacuum gap required for the access of neutral beam ports and other diagnostics near the outboard mid-plane. Extensive calculations are carried out on the plasma beta limits for low-n (n being toroidal mode number) MHD modes in several major operating regimes. The results lead to a practical and optimistic design point: plasma-wall separation ≈ 10 cm, and the outboard gap having a vertical separation of about 80 cm between the upper and lower plates. This is one of the choices that will make it feasible to achieve the advanced operation with bootstrap current fraction of over 80% at $\beta_n = 5$ in the reversed shear mode in KSTAR.

Keywords: Stabilizer; Magnetohydrodynamic stability; Parametric study

1. Introduction

The proposed Korea Superconducting Tokamak Advanced Research (KSTAR) tokamak [1] will be a versatile facility capable of operating in a wide range of operating modes. The physics goals of the KSTAR program require a machine with considerable flexibility in an operating space in l_i and β_n: $l_i(3)$ from 0.4 to 1.3, and β_n of 1.5–5. Here $l_i(3) = 2\int B_p^2 \, dV/[R_0(\mu_0 I_p)^2]$ and $\beta_n \equiv \beta aB/I_p$, where B_p *is* the poloidal magnetic field, R_0 is the plasma major radius, I_p is the plasma current, a is the plasma minor radius, and B is the toroidal field. In KSTAR, it is planned that $R_0 = 1.8$ m,

* Corresponding author. Tel.: +82-42-869-8184; fax: +82-42-869-8190.

E-mail address: dylee@sorak.kaist.ac.kr (D.-Y. Lee)

0920-3796/99/$ - see front matter
PII: S0920-3796(99)00060-5

$a = 0.5$ m, $I_p \leq 2$ MA, $B \leq 3.5$ T. The upper limit on β_n of 5 represents a challenging goal for steady-state tokamak operation. If KSTAR is successful in achieving such performance, it would be a significant breakthrough in the physics basis for high-performance, continuously-operating tokamak reactors. A lower limit of $\beta_n = 1.5$ for steady-state operation is set to avoid the cost of designing the machine for steady-state operation at uninterestingly low beta values. The required range in $l_i(3)$ for steady-state operation (0.4–1.3) spans the range of expected high-β_n scenarios, from 'reversed shear' to 'high-l_i' plasma configurations. One of the major missions of the KSTAR machine will be to explore and compare these different tokamak-operating regimes. During the design phase of the KSTAR tokamak, extensive analysis has been performed to insure and to verify that the poloidal field system, the configurational details, and the heating and current-drive systems are adequate to produce the range of the tokamak discharges that will be of interest for experimental study and demonstration. Furthermore, the KSTAR facility is aiming at the long pulse operation. It is initially designed for about 20-s deuterium pulses at 15-min intervals, up to a maximum of 50 per day. With upgrades, it will provide 300-s pulses. One key engineering component that is necessary in realizing such missions is the passive plates stabilizer around the plasma surface. It is the main objective of this paper to study the effect of the passive stabilizer on the magnetohydrodynamic (MHD) stability of the KSTAR plasma and to provide a guide to its design.

The performance of an advanced tokamak plasma like that of KSTAR can be critically dependent on the separation between the plasma and its adjacent hardware. Its stability may be determined by the distance from the plasma surface to the passive stabilizer, about which we will present much more later, heat and particle exhaust depends on how and where the divertor field lines intersect the divertor structure, radio-frequency wave coupling depends on the plasma–launcher separation, and control of particle sources depends on avoiding unintended plasma-material contact. In particular, careful control of the plasma shape and design of the passive plates position is essential for high performance of the machine. The necessity of the plates is primarily for fast-time scale vertical position control and for stabilization of the non-axisymmetric MHD instabilities, most importantly the external kink instability.

Fast vertical position control is needed to stabilize the vertical instability and maintain the vertical plasma position within 1 cm of its normal location in the presence of spontaneous disturbances. The vertically elongated plasma can be easily unstable to a vertical displacement. Since KSTAR plasma will have an elongation of $\kappa_x = 2.0$ with a triangularity $\delta_x = 0.8$, control of the instability is a major concern that has to be resolved. The primary role of the passive structure is to reduce the vertical instability growth rate so as to make active control feasible. In conjunction with the plates, normal-conducting coils inside the KSTAR vacuum vessel will be provided for position control on fast time scales (10–20 ms). The detailed result of extensive design calculations for this issue as well as the radial position control can be found elsewhere [2].

Advanced high-β_n tokamak plasma configurations can be limited by low-n (n, the toroidal mode number) non-axisymmetric MHD instabilities such as the external kink mode. Learning how to stabilize such modes is an important area of physics research for KSTAR. Generally, MHD instabilities are dependent on details of the plasma pressure and current density profiles, the plasma boundary shape, and the boundary conditions such as the presence of the external walls. Stabilization of the internal modes such as the ballooning mode may be done solely by profile control in KSTAR. The external kink, on the other hand, is by definition always subject to a surface perturbation, although it also has a significant displacement inside when the plasma beta is high enough. Stability of this mode is most sensitive to the condition of the external stabilizing wall, especially when the equilibrium current profile is thick. Typically, worse stability to the kink mode is anticipated for plasma with a thicker current density profile, and this is in fact the case for the reversed shear equilibria. In this case,

presence of the external wall is quite critical [3] since the reversed shear generically has a thick current profile. The vacuum vessel is a passive structure, but it is too distant in KSTAR to have any stabilizing effect on the kink mode. It is therefore very likely, as we demonstrate further later, that stabilization by closely fitting additional external plates will be part of any successful strategy in KSTAR. Their final positioning will be determined by a balance of vertical stability and kink mode stabilization together with impurity control considerations. Therefore, quantitative estimation for optimistic design of such plates is necessary from kink mode analysis. We present the result of such work here. This paper summarizes the result of parametric, numerical computations in terms of the separation distance of the plates from the plasma surface as well as in terms of the vacuum gap size on the outboard side. Mainly, the effect of such variables on the plasma β_n limits for low-n ($n = 1$–5) MHD modes in several practical as well as leading operating regimes is investigated.

2. Separation distance and gap size of the plates

The KSTAR plasma equilibria are created by the JSOLVER equilibrium code [4]. This is a highly accurate, flux-coordinate, fixed-boundary equilibrium code. The plasma boundary is determined by $x = R + a\cos(\theta + \delta\sin\theta)$ and $z = \kappa a \sin\theta$, with the parameters $R = 1.8$ m, $a = 0.5$ m, $\kappa = 1.8$, which is regarded as κ_{95} (the elongation at 95% flux surface), and $\delta = 0.5$, which is likewise δ_{95}. Free input functions are the plasma pressure and current density functions, for which we use some analytic functional forms for convenience. For such given equilibria, the stability to ideal MHD modes is analyzed by using the PEST II [5] linear stability code. These modes are conveniently distinguished by their toroidal mode number, n. In this work, we consider low-n modes, $n = 1$–5, as well as the infinite n ballooning mode. The external kink usually corresponds to the $n = 1$ mode with a finite surface perturbation. This mode often becomes one of the most dangerous instabilities in tokamaks. Stabilizing the external kink instability can be effectively done by invoking an external conducting wall close to the plasma surface. For higher n modes, internal contribution becomes more significant. Thus, wall stabilization may be less effective, but rather careful profile control will be needed for good stability to these higher n modes.

The KSTAR facility is planned to have the passive plates close to the plasma surface inside the vacuum vessel. However, those plates will have to cover only the poloidally-limited area to avoid engineering conflicts. In particular, the outboard side must be allowed to have some vacuum gap for the access of neutral beams ports and other diagnostics. In high-β deformed plasma, however, the outboard side is the most contributing region to development of the instabilities. Thus, covering the outboard side over a sufficient portion as much as possible is crucial to the effectiveness of wall stabilization. The KSTAR plates may be simulated using the VACUUM code [6] in conjunction with PEST II. In the code, the plate shapes shown in Fig. 1 are possible. The walls used in the simulation are assumed to be ideal perfectly conducting. This is of course unrealistic, and a discussion on this issue will be given in the final section. For KSTAR plates, either shape (a) or (b) in Fig. 1 is appropriate. Shape (a) perfectly models the vacuum gap on outboard side. Although it models unrealistically the inboard side where no stabilizing material will exist in the actual device, we will see that the inboard side has practically no impact on the stability in high-β plasma. One may use shape (b), which correctly models the inboard side. The outward bulge approximately mimics the outboard vacuum gap as long as its horizontal length is long enough. After extensive calculations, we have verified that the two shapes (a) and (b) in fact give almost the same results in the stability calculation. We therefore use shape (a) in most of the calculations for convenience.

In order to investigate the relative effects of introducing a mid-plane gap in the conducting wall on the outboard and inboard sides of the plasma, we performed two series of calculations, where we monitored the unstable growth rate of the $n = 1$ external mode as we changed the out-

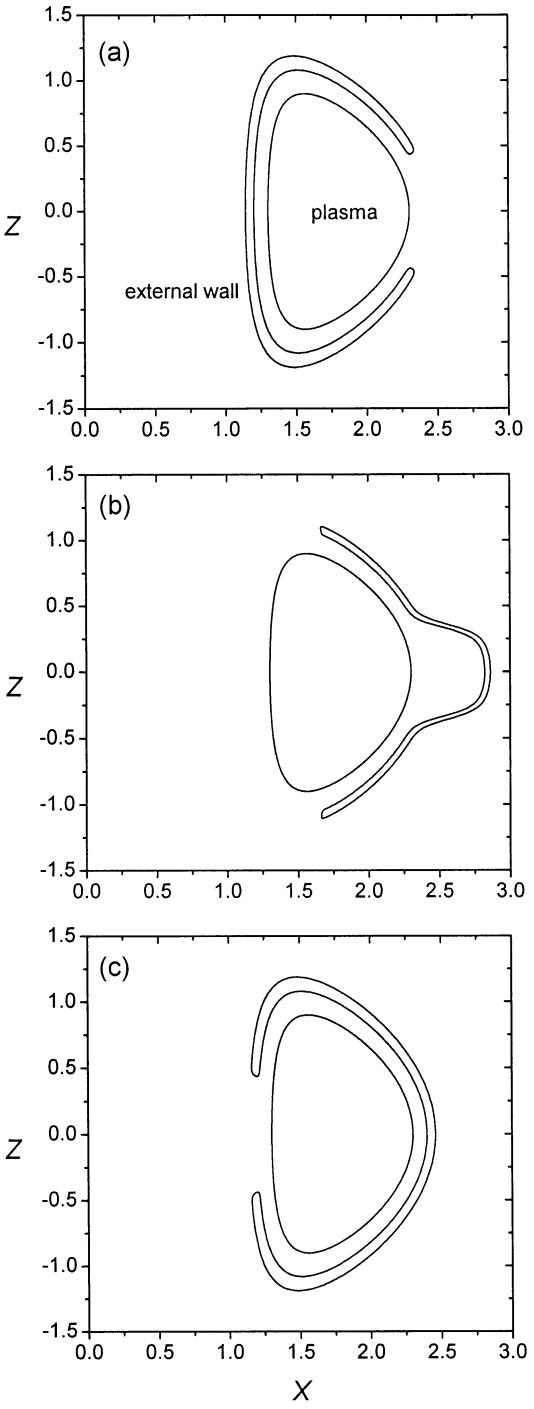

Fig. 1. External wall shapes that can be used to simulate the passive plates or vacuum vessel in the PEST II-VACUUM code system.

board and inboard gap angle. The result is shown in Fig. 2. We started with a plasma that was just barely unstable when surrounded by a full conformal conducting wall with a plasma-wall separation of $0.5a$. The plasma has $\beta_n = 4.0$ and $q_{\text{edge}} = 3.7$. For the wall with the outboard gap as in Fig. 1(a), the gap angle is defined to increase away from the outboard mid-plane. As the gap angle increases, the squared growth rate, w^2, normalized to that with no wall, rapidly increases, reaching nearly unity at around 90° (curve with circles in Fig. 2). For the wall with the inboard gap, using the shape (c) of Fig. 1, the gap angle is taken to increase away from the inboard mid-plane. The curve with squares in Fig. 2 indicates that w^2(full wall)/w^2, where w^2(full wall) is the growth rate with a full conformal wall, stays close to unity until the inboard gap opens up to 80°, and then decreases rapidly as the gap becomes wider. The two curves imply that the inboard side is practically irrelevant in determining $n = 1$ mode stability.

Using shape (a) in Fig. 1, we have quantitatively tested the effect of the gap size and plasma-wall separation distance on the stability limit in terms of critical β_n values. Fig. 3 shows the β_n limit for the $n = 1$ external mode over a practical range in outboard gap angle, from about 30 to 60°, in the high-β conventional mode (where $q_0 = 1.05$, $q_{\text{edge}} \sim 4$; see further discussion in the next section). Here the gap angle is referred to as half of the total gap size, being defined to increase away from the outboard mid-plane as already indicated. A gap size that is smaller than about 36° seems unrealistic due to the interference with diagnostic ports. The two main curves are for wall distances of $0.2a$ (10 cm) and $0.3a$ (15 cm), respectively. The β_n limits for a complete conformal wall at $0.3a$ and for the case with no wall are also shown for comparison. Above each curve is the unstable domain and vice versa. Certainly, having a wider gap for a given plasma–wall distance decreases the maximum stable β_n. However, the effect is less significant compared with that in the reversed shear mode (see further discussion in the next section), as shown in Fig. 4 where similar calculation results are plotted. Overall, the effect of both the gap size and plasma–wall distance is

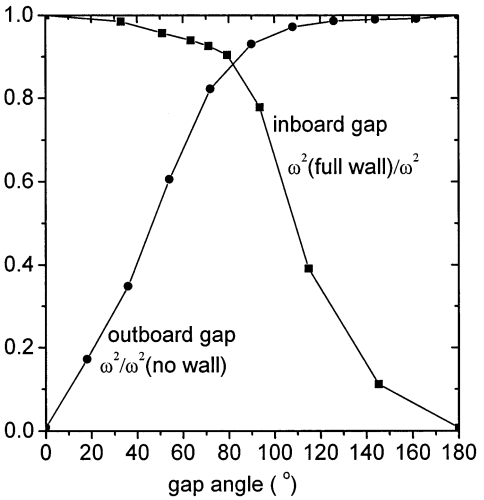

Fig. 2. Comparative study of the relative effects of inboard and outboard gaps on the stability in terms of squared growth rate w^2.

more significant than in the previous case. This is due to the fact that the current density profile is thicker in the reversed shear equilibria than in the conventional mode equilibria, where the safety factor q profile is monotonic. In order to achieve the high β_n with the unavoidable outboard gap, therefore, the plates should be placed sufficiently close to the plasma surface. For the same reversed

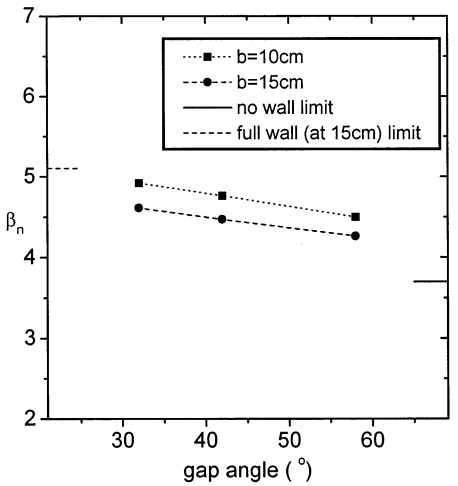

Fig. 3. β_n limit for $n=1$ mode versus gap angle for a conventional safety factor q profile. b is the plasma-wall separation distance.

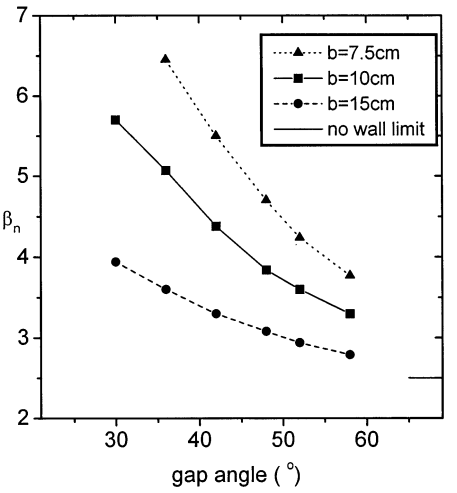

Fig. 4. β_n limit for $n=1$ mode versus gap angle for three different plasma–wall distances for reversed shear q profile equilibria. The limit with no wall is also shown as a solid line.

shear equilibria, the effects on other toroidal mode number instabilities are described in Fig. 5. Calculations are done for several cases with various values of plasma–wall distance and gap size angle. Two features are clearly seen from the figure. First, the $n=1$ mode is the most unstable one, giving the lowest β_n limit in all cases. Higher stability is achieved for higher n modes. Secondly, wall stabilization is most effective for the $n=1$

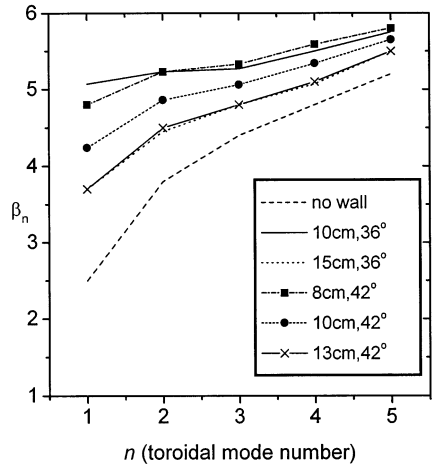

Fig. 5. The effect of the gap size and plasma–wall distance on the β_n limit of $n=1$–5 modes in the same reversed shear configuration as in Fig. 4.

mode. This is because the higher n modes tend to have less external contribution than does the $n=1$ mode. The reversed shear mode is discussed further in the next section, where we will use the design option (10 cm, 36°): this will be a practical and optimistic choice for the physics requirement for the advanced tokamak operation in KSTAR.

3. Effect on various operating modes

As discussed earlier, one of the primary missions of the KSTAR will be to explore and compare different operating modes. We have identified four major operating scenarios here for which the effect of the passive plates on the stability was quantitatively computed in a similar way as already discussed. The four modes are (i) conventional mode, (ii) high-β conventional mode, (iii) high bootstrap-fraction mode, and (iv) reversed shear mode. Separate discussions on each mode follows.

In the following presentations, corresponding to Figs. 6–9, the stability analysis was done for $n=1$–5 modes as well as for the infinite n ballooning mode. The KSTAR external wall (i.e. the passive plates) was simulated by using shape (a) of Fig. 1 with a gap angle of 36° (corresponding to vertical separation of about 80 cm between the upper and lower plates) and the plasma–wall distance of $0.2a$ (hereafter, we will call this the KSTAR partial wall). For each operating mode, the plasma pressure and current density profiles in equilibrium were extensively varied in order to optimize the maximum stable β_n. The bootstrap current was also computed, and the constraint for the perfect alignment with the total (desired) current profile was imposed in the stability limit search [7].

3.1. Conventional mode

This is one of the practical and conventional operating modes. The q profile is monotonic from the magnetic axis to the plasma edge, and q at axis, q_0, *is* set to be slightly less than unity, about 0.95, since that is often the case in actual experiments. This usually causes the $n=1$ 'internal' kink and the Mercier instabilities unless the plasma pressure profile, in particular, near the magnetic axis, is carefully chosen. The stability result in Fig. 6 is obtained by carefully tailoring the pressure profile in such a way that it is as flat as possible near the magnetic axis where q is less than unity (plot (b) in Fig. 6). The β_n limit for $n=1$ external mode is significantly increased from 3.8 with no wall up to 6.2 with the KSTAR partial wall. There are also increments for $n=2$–5 modes, although less significantly. However, these β_n limits are, even with no wall, already above the ballooning limit ($\beta_n=3.4$), for which the wall stabilization is irrelevant. Therefore, in

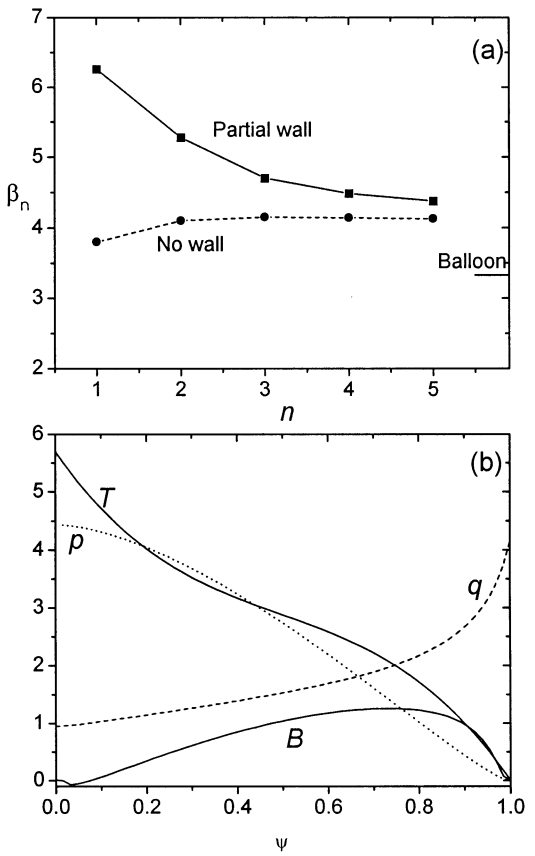

Fig. 6. (a) β_n limit of the $n=1$–5 and ballooning (designated by Balloon) modes in conventional operating mode. 'Partial wall' represents the wall shape of Figure l(a). (b) Typical equilibrium profiles of pressure (p), safety factor (q), total current density (T), and bootstrap current density (B) at $\beta_n=3.5$ where the bootstrap fraction $f_{bs}\sim 30\%$.

this operating mode, the external wall has no practical impact. This situation is due to the peculiar choice of the pressure profile to avoid the internal kink and Mercier instabilities.

3.2. High-β conventional mode

In this mode, the q profile is still monotonic, but q_0 is now set to about 1.05. Thus, one can avoid the internal kink and Mercier instabilities. Then a steeper pressure profile can be tried which may lead to higher stable β_n. In fact, using the profiles in Fig. 7(b), the ballooning stability is improved, $\beta_n = 4.0$ in Fig. 7(a). The limiting β_n is given by the $n = 1$ external mode when no wall is present: $\beta_n = 3.8$. This is increased up to 4.9 by the partial wall, which is above the ballooning

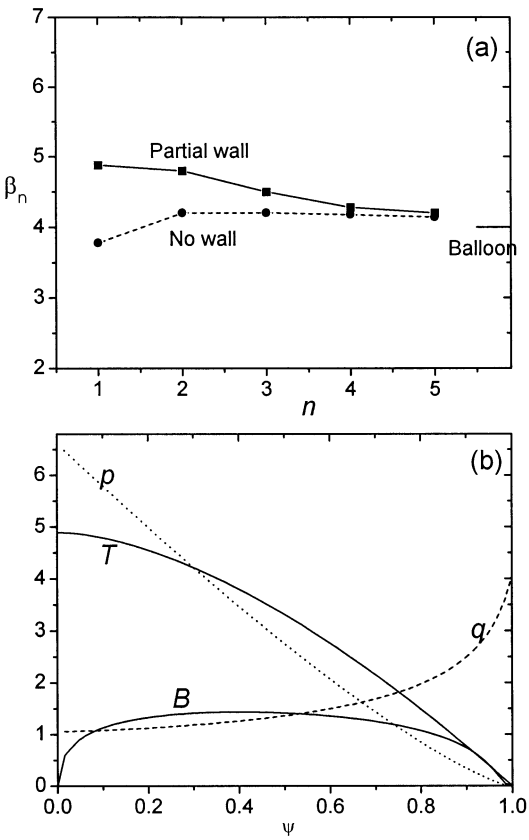

Fig. 7. (a) β_n limit of the $n = 1$–5 and ballooning modes in high-β conventional operating mode. (b) Similar plot as in Fig. 6. $\beta_n = 3.9$ where the bootstrap fraction $f_{bs} \sim 42\%$.

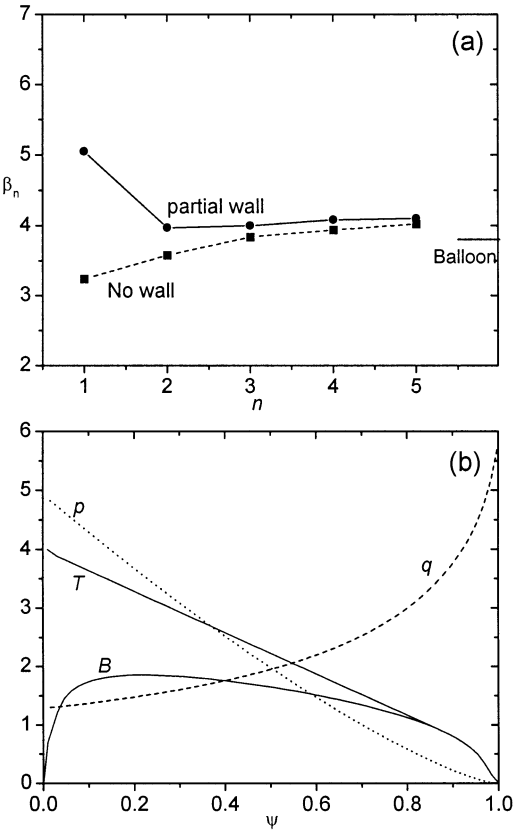

Fig. 8. (a) β_n limit of the $n = 1$–5 and ballooning modes in high bootstrap-fraction operating mode. (b) Similar plot as in Fig. 6. $\beta_n = 3.8$ where the bootstrap fraction $f_{bs} \sim 65\%$.

limit. The same wall also increases β_n limits for other n modes above the ballooning limit. Therefore, implementing the wall is practical in this operation scenario and makes possible the β_n of up to 4.0 set by the ballooning mode.

3.3. High bootstrap-fraction mode

This is similar to the ARIES-I mode [8]. It is characterized by much higher bootstrap current fraction than in the previous two cases, hence the name 'high bootstrap-fraction' mode. This can be achieved by lowering the total plasma current, which was 2 MA in the previous two cases, down to 1.5 MA, leading to a larger β_p, the poloidal beta. It is in turn proportional to the bootstrap current fraction [9]: a fraction of about 65% at

$\beta_n = 3.8$ was obtained (Fig. 8(b)). The q values are overall raised with a q_0 of 1.3. The stability with no wall is rather degraded by these profiles, as shown in Fig. 8(a). However, the partial wall plays a key role in enhancing the limits above the ballooning limit. In brief, with the wall in this mode, β_n of 3.8 set by the ballooning mode is possible with a bootstrap current fraction of 65%.

3.4. Reversed shear mode

The advanced tokamak concept is characterized by three ingredients: high confinement, high-β, and a large, well-aligned bootstrap current fraction. The reversed shear equilibria may be a strong candidate that meets all three conditions [3,10]. This will definitely be one of the primary operating modes in KSTAR. As shown in Fig. 9(b), the q profile is non-monotonic with a central region of negative shear due to a hollow current density profile. Such a hollow current profile naturally resembles that provided by the bootstrap current, thus leading to very good alignment. Also, since the ballooning is in the second stability regime in the negative shear region, this allows a quite steep pressure gradient there. This leads to a very high β_n limit for the ballooning mode, over 5.7 as shown in Fig. 9(a). However, since the current profile is generically broad in this reversed shear equilibrium, the stability to the $n = 1$ external kink mode gives a very low β_n limit, $\beta_n = 2.5$, when no wall stabilization is invoked. As already stated in the previous section, the wall can greatly increase this limit: from 2.5 up to about 5, where the bootstrap fraction of over 80% is calculated to be possible. The enhancement for other n modes is also substantial. Therefore, the presence of the KSTAR wall is essential in achieving this advanced operating mode, and the present choice of design values, plasma–wall distance of 10 cm and gap angle of 36° (vertical separation of about 80 cm), is quite effective for this purpose.

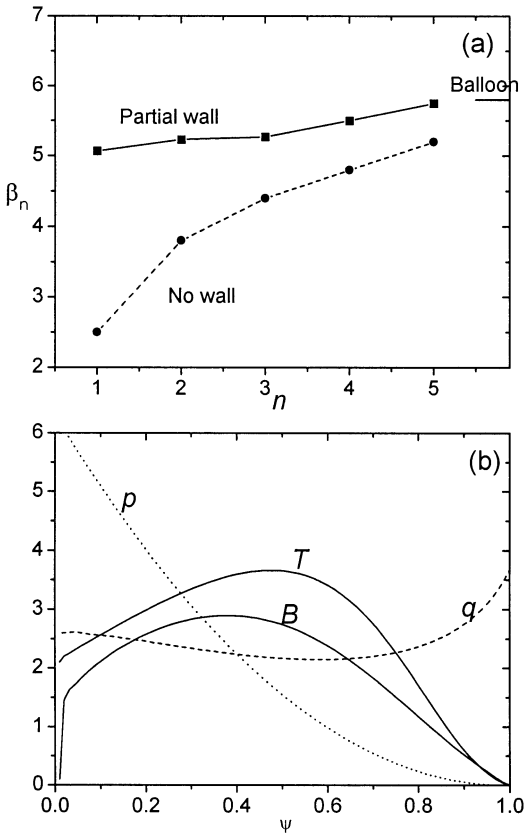

Fig. 9. (a) β_n limit of the $n = 1$–5 and ballooning modes in reversed shear operating mode. (b) Similar plot as in Fig. 6. $\beta_n = 5$ where the bootstrap fraction $f_{bs} \sim 80\%$.

4. Summary and discussion

In this work, we have computed numerically and quantitatively the effect of the KSTAR passive plates on the MHD stability limit. The study was done in order to guide the design activity of the plates by testing various cases with different gap sizes of the plates on the outboard side and with different plasma–wall separation distances. Also, the investigation was done for various operating modes including the reversed shear mode. It is confirmed that a close fit of the passive plates will be quite necessary in order to realize the advanced operating modes like the reversed shear. For example, the plate structure with gap angle of 36° (vertical separation of about 80 cm) and plasma–wall distance of about 10 cm will be a quite optimistic design for such a purpose. This plate structure is found to be effective enough for other operating modes as well.

We should remark that our study was based on at least two assumptions. One is that the passive plates are assumed to be toroidally continuous while they have poloidal vacuum gap. This is not realistic since in KSTAR at least one toroidal break in the plates is necessary to decouple the plates from the Ohmic system during the plasma start-up. However, as long as the gap associated with the toroidal break is not too large, it is intuitively obvious that the stability results will not change much. Second, it was assumed that the plates would be perfectly conducting. This is by no means true, and the actual plates will be resistive, being made of GLIDCOP (resistivity = 2.6×10^{-8} Ω m) with thickness of about 2.5 cm. This will allow the helical flux loss through the plates. Then it leads to the resistive wall mode (RWM) [11,12], a modified kink mode, which would grow on a wall penetration time scale. The growth rate is fairly slow compared with the ideal MHD time scales. However, it will still be a major concern for long-pulse high-β steady-state operations in future advanced machines such as the KSTAR and ITER. Currently, several schemes are available for control of the ROOM. One is to use the plasma rotation [13–16] at some sufficient rate in conjunction with the resistive wall. This may be realistic using the planned input power of neutral beam injection (NBI) in KSTAR. Another possible way to stabilize the RWM is to properly mount a system of active feedback coils behind the passive plates (and perhaps on the gap region between the plates) in order to compensate for the helical flux leakage through the plates [12,17–19]. The current plan is to add this in KSTAR as a future upgrade. In both methods, the existence and role of the passive plates are essential.

One final remark is that we have considered here only the double-null (DN) up–down symmetric plasmas. The KSTAR PF coil system is being designed to have a capability to generate a single-null (SN) plasma as well. The SN plasma will, however, be substantially up–down non-symmetric. This further deformation of the plasma shape can affect the stability analysis to some extent [20]. There is, however, no doubt that the external wall will still be a good stabilizer, although its design is being optimized for a DN plasma based on the calculation result of the present paper. Stability analysis is more difficult for KSTAR SN plasma because of the numerical difficulty for the severely deformed SN plasma. This issue is under investigation and the result will be reported elsewhere.

Acknowledgements

This work was supported by the Korea Basic Science Institute under the Korea Superconducting Tokamak Advanced Research project. We are grateful to the KSTAR team for helpful comments and for continuous support and encouragement.

References

[1] D.I. Choi, G.S. Lee, J. Kim, H.K. Park, C.S. Chang, et al., The KSTAR tokamak, in Proceedings of the 17th IEEE/NPSS Symposium Fusion Engineering, Vol 1, San Diego, CA, 6–10 October 1997, pp. 215–220.

[2] H. Jhang, C. Kessel, N. Pomphrey, S.C. Jardin, G.S. Lee, C.S. Chang, Design calculations for fast plasma position control in Korea Superconducting Tokamak Advanced Research, Fusion Eng. Des. 45 (1999) 101.

[3] C. Kessel, J. Manickam, G. Rewoldt, W. Tang, Improved plasma performance in tokamaks with negative magnetic shear, Phys. Rev. Lett. 72 (1994) 1212.

[4] J. Delucia, S.C. Jardin, A.M.M. Todd, An iterative metric method for solving the inverse tokamak equilibrium problem, J. Comput. Phys. 37 (1980) 183.

[5] R.C. Grimm, R.L. Dewar, J. Manickam, Ideal MHD stability calculations in axisymmetric toroidal coordinate systems, J. Comput. Phys. 49 (1983) 94.

[6] M.S. Chance, Vacuum calculations in azimuthally symmetric geometry, Phy. Plasmas 4 (1997) 2161.

[7] J. Manickam, M.S. Chance, S.C. Jardin, C. Kessel, D. Monticello, N. Pomphrey, A. Reiman, C. Wang, L.E. Zakharov, The prospects for magnetohydrodynamic stability in advanced tokamak regimes, Phys. Plasmas 1 (1994) 1601.

[8] F. Najmabadi and the ARIES team, The ARIES-I Tokamak Reactor Study-Final Report, Report UCLA-PPG-1323, Vol. 2, University of California, Los Angeles, 1991.

[9] C.E. Kessel, The bootstrap current in a tokamak, Nucl. Fusion 34 (1994) 1221.

[10] A.D. Turnbull, T.S. Taylor, Y.R. Lin-Liu, H. St. John, High beta and enhanced confinement in a second stable core VH-mode advanced tokamak, Phys. Rev. Lett. 74 (1995) 718.

[11] C.G. Gimblett, On the free boundary instabilities induced by a resistive wall, Nucl. Fusion 36 (1986) 617.
[12] C.M. Bishop, An intelligent shell for the toroidal pinch, Plasma Phys. Control. Fusion 31 (1989) 1179.
[13] A. Bonderson, D.J. Ward, Stabilization of external modes in tokamaks by resistive walls and plasma rotation, Phys. Rev. Lett. 72 (1994) 2709.
[14] N. Pomphrey, S.C. Jardin, J. Bialek, et al., MHD regimes and feedback stabilization in advanced tokamaks, in Plasma Physics and Controlled Nuclear Fusion Research 1994, Proceedings of the 15th International Conference, Serville, International Atomic Energy Agency, Vienna, 1996, Vol. 3, p. 251.
[15] D.-Y. Lee, Resistive wall mode in rotating plasma with multiple walls, Phys. Plasmas 5 (1998) 4098.
[16] A. Bonderson, C.G. Gimblett, R.J. Hastie, Resistive wall mode stabilization in toroidal geometry, Phys. Plasmas 6 (1999) 637.
[17] R. Fitzpatrick, T.H. Jensen, Stabilization of the resistive wall mode using a fake rotating shell, Phys. Plasmas 3 (1996) 2641.
[18] T.H. Jensen, R. Fitzpatrick, Resistive wall feedback stabilization, Phys. Plasmas 4 (1997) 2997.
[19] D.-Y. Lee, M.S. Chance, J. Manickam, N. Pomphrey, M. Okabayashi, Two-dimensional calculation of eddy currents on external conducting walls induced by low-e external modes, Phys. Plasmas 5 (1998) 735.
[20] A.D. Turnbull, T.S. Taylor, M.S. Chu, R.L. Miller, Y.R. Lim-Liu, Synergism between cross-section and profile shaping in beta optimization of tokamak equilibria with negative central shear, Nucl. Fusion 38 (1998) 1467.